Ranging Precision Analysis of LTE Signals

Kimia Shamaei, Joe Khalife, and Zaher M. Kassas
Department of Electrical and Computer Engineering
University of California, Riverside, USA
Emails: kimia.shamaei@email.ucr.edu
jkhalife@ece.ucr.edu, zkassas@ieee.org

***Abstract*—The ranging precision of the secondary synchronization signal in cellular long-term evolution (LTE) systems is evaluated. First, the pseudorange error for a delay-locked loop with a coherent baseband discriminator is analyzed, and a closed-form expression for the standard deviation of the pseudorange error is derived. Second, the effect of multipath on the ranging error is evaluated analytically. Experimental results closely matching the analytical expression of the pseudorange error standard deviation are presented. Key remarks to take into consideration when designing a receiver for positioning using LTE signals are provided throughout the paper.**

I. Introduction

Cellular signals are attractive for positioning due to their ubiquity, geometric diversity, high received power, and large bandwidth [1]. Recent research have demonstrated how cellular signals could be used for localization: (1) in a standalone fashion [2], [3] or (2) as an aiding source for an inertial navigation system in the absence of global navigation satellite systems (GNSS) signals [4], [5]. Moreover, cellular signals could be fused with GNSS signals, when available, to improve the positioning accuracy [6], [7].

Long-term evolution (LTE) – the transmission standard of the fourth generation cellular system – is particulary attractive for positioning. The potential of LTE signals for navigation has been recently demonstrated [8]–[10], and the literature on LTE-based navigation has shown several experimental results for positioning using real LTE signals [11]–[14]. Moreover, several software-defined receivers (SDRs) have been proposed for navigation with real and laboratory-emulated LTE signals [15]–[17], and experimental results with real LTE signals using these SDRs showed meter-level accuracy [11], [17].

There are three possible reference sequences in a received LTE signal that can be used for navigation: (1) primary synchronization signal (PSS), (2) secondary synchronization signal (SSS), and (3) cell-specific reference signal (CRS). The PSS is expressible in only three different sequences, each of which represents the base station (also known as Evolved Node B or eNodeB) sectors' ID. This presents two main drawbacks: (1) the received signal is highly affected by interference from neighboring eNodeBs with the same sector ID and (2) the user equipment (UE) can only simultaneously track a maximum of three eNodeBs, which becomes inefficient in an environment with more than three eNodeBs. The SSS is expressible in only 168 different sequences, each of which represents the cell group identifier, or group ID; therefore, it does not suffer from the aforementioned drawbacks of the PSS. Using conventional computationally inexpensive delay-locked loops (DLLs), relatively precise pseudorange measurements can be obtained from the SSS. Moreover, the transmission bandwidth of the SSS is 930 KHz, leading to a comparable ranging precision as in GPS, whose C/A bandwidth is 1.023 MHz; however, and similar to GPS, the SSS is susceptible to multipath. The third reference sequence is the CRS, which is mainly transmitted to estimate the channel between the eNodeB and the UE. It has been shown that estimating the time-of-arrival (TOA) using the CRS is more robust in multipath environments due to its higher transmission bandwidth [9], [18]. However, the CRS is scattered in both frequency and time and is transmitted from all transmitting antennas; hence, conventional DLLs cannot be used for tracking the CRS. The focus of this paper is on analyzing the ranging precision with the SSS.

LTE systems transmit using orthogonal frequency division multiple access (OFDMA), which is considerably different than code-division multiple access (CDMA) – the transmission standard for GPS. The ranging precision for GPS signals has been extensively studied analytically and empirical error budgets have been established [19]. Although positioning performance with SSS signals has been evaluated experimentally, the SSS ranging precision has not been studied analytically.

This paper makes two contributions. First, the SSS ranging precision using a DLL with a coherent baseband discriminator in the presence of additive white noise is analyzed and a closed-form expression for the standard deviation of the ranging error is derived. Second, the effect of multipath on the ranging accuracy is analyzed numerically. Experimental results are provided to validate the theoretical expression of the ranging error standard deviation.

The remainder of this paper is organized as follows. Section II discusses the received SSS model and the architecture of the DLL. Section III provides open-loop and closed-loop analyses to derive a closed-form expression for the statistics of the resulting ranging error in a coherent baseband discriminator. Section IV studies the effect of multipath on the output of a coherent baseband discriminator. Section V demonstrates experimental results closely matching the analytical expression for the ranging error standard deviation.

II. Signal Model and Tracking Loops

LTE signals are divided into frames of $T_{sub} = 10$ ms, where each frame consists 20 slots [20]. The UE uses two synchronization signals transmitted by the eNodeB in each frame,

ISBN 978-0-9928626-7-1

namely the PSS and the SSS, to acquire the frame start time. The PSS can be one of three different orthogonal sequences, which is determined by the sector ID of the eNodeB. The SSS can be one of 168 different orthogonal sequences, which is determined by the group ID of the eNodeB. It is worth noting that tracking the SSS allows the UE to track signals from more than three eNodeBs [17]. The SSS is transmitted only once in each frame, either in slot 0 or 10, and occupies the 62 middle subcarriers out of N_c total subcarriers. The value of N_c can be assigned to 128, 256, 512, 1024, 1536, or 2048. The rest of the subcarriers within the same symbol in which the SSS is transmitted are set to be zero-valued. Therefore, it is possible to obtain the time-domain equivalent of the SSS by taking its inverse Fourier transform (IFT), given by

$$s_{SSS}(t) = \begin{cases} \text{IFT}\{S_{SSS}(f)\}, & \text{for } t \in (0, T_{symb}), \\ 0, & \text{for } t \in (T_{symb}, T_{sub}), \end{cases}$$

where $S_{SSS}(f)$ is the SSS sequence in the frequency-domain [20], $T_{symb} = 1/\Delta f$ is the duration of one symbol, and $\Delta f = 15$ KHz is the subcarrier spacing in LTE systems.

The received signal after the receiver's radio frequency front-end is processed in blocks each of which spans one frame, which can be modeled as

$$\begin{aligned} r(t) = \sqrt{C} e^{j(2\pi \Delta f_D t + \Delta\phi)} \\ \times [s_{code}(t - t_{s_k} - kT_{sub}) + d(t - t_{s_k} - kT_{sub})] + n(t), \\ \text{for } kT_{sub} \le t \le (k+1)T_{sub}, \quad k = 0, 1, 2, \cdots, \end{aligned}$$

where $s_{code}(t) \triangleq \sqrt{\frac{T_{sub}}{W_{SSS}}} s_{SSS}(t)$, $W_{SSS} = 930$ KHz is the SSS bandwidth, C is the received signal power including antenna gains and implementation loss, t_{s_k} is the true TOA of the SSS signal, $\Delta\phi$ and Δf_D are the residual carrier phase and Doppler frequency, respectively, $n(t)$ is an additive white noise with constant power spectral density $N_0/2$ Watts/Hz, and $d(t)$ is some data other than the SSS transmitted by the eNodeB, where

$$d(t) = 0 \quad \text{for } t \notin (t_{s_k}, t_{s_k} + T_{symb}).$$

The tracking loop is composed of two components, namely a frequency-locked loop (FLL)-assisted phase-locked loop (PLL) and a rate-aided DLL. Two types of discriminators can be considered for a DLL: (1) coherent and (2) noncoherent [19], [21]. Coherent discriminators can be used when the carrier phase is known by the receiver. Noncoherent discriminators are independent of the carrier phase tracking accuracy (e.g., the dot-product discriminator or the early-power minus late-power discriminator). In this paper, it is assumed that the residual carrier phase and Doppler frequency are negligible, i.e., $\Delta\phi \approx 0$ and $\Delta f_D \approx 0$. Therefore, a coherent baseband discriminator may be used in the DLL. Fig. 1 represents the structure of a coherent DLL that is used for tracking the code phase [22]. In what follows, the ranging precision of the DLL shown in Fig. 1 is evaluated.

In the DLL, the received signal is first correlated with the early and late locally-generated replicas of the SSS. The

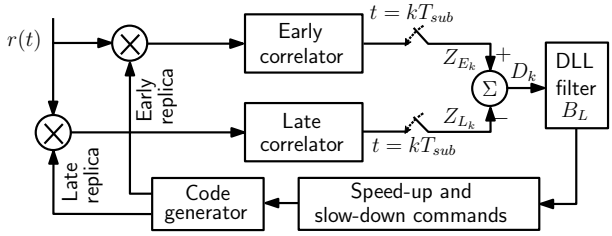

Fig. 1. Structure of a DLL employing a coherent baseband discriminator to track the code phase.

resulting early and late correlations are given by

$$\begin{aligned} Z_{E_k} &= \frac{1}{T_{sub}} \int_{kT_{sub}}^{(k+1)T_{sub}} r(t) s_{code}(t - \hat{t}_{s_k} + \frac{t_{eml}}{2} T_c - kT_{sub}) dt \\ &\triangleq S_{E_k} + N_{E_k}, \\ Z_{L_k} &= \frac{1}{T_{sub}} \int_{kT_{sub}}^{(k+1)T_{sub}} r(t) s_{code}(t - \hat{t}_{s_k} - \frac{t_{eml}}{2} T_c - kT_{sub}) dt \\ &\triangleq S_{L_k} + N_{L_k}, \end{aligned}$$

where $T_c = 1/W_{SSS}$ is the chip interval, t_{eml} is the correlator spacing (early-minus-late), and $\hat{t}_{s_k}$ is the estimated TOA. The signal components of the early and late correlations, S_{E_k} and S_{L_k}, respectively, are given by

$$S_{E_k} = \sqrt{C} R\left(\Delta\tau_k - \frac{t_{eml}}{2} T_c\right), \; S_{L_k} = \sqrt{C} R\left(\Delta\tau_k + \frac{t_{eml}}{2} T_c\right),$$

where $\Delta\tau_k \triangleq \hat{t}_{s_k} - t_{s_k}$ is the propagation time estimation error and $R(\cdot)$ is the autocorrelation function of $s_{code}(t)$, given by

$$\begin{aligned} R(\Delta\tau) &= \frac{1}{T_{sub}} \int_0^{T_{sub}} s_{code}(t) s_{code}(t + \Delta\tau) dt \\ &= \text{sinc}(W_{SSS}\Delta\tau) - \frac{\Delta f}{W_{SSS}} \text{sinc}(\Delta f \Delta\tau) \\ &\approx \text{sinc}(W_{SSS}\Delta\tau). \end{aligned}$$

It can be shown that the noise components of the early and late correlations, N_{E_k} and N_{L_k}, respectively, are zero mean with the following covariances [22]

$$\text{var}\{N_{E_k}\} = \text{var}\{N_{L_k}\} = \frac{N_0}{2T_{sub}}, \qquad \forall k$$

$$\mathbb{E}\{N_{E_k} N_{L_k}\} = \frac{N_0 R(t_{eml} T_c)}{2T_{sub}}, \qquad \forall k$$

$$\mathbb{E}\{N_{E_k} N_{E_j}\} = \mathbb{E}\{N_{L_k} N_{L_j}\} = 0, \quad \forall k \neq j.$$

III. Statistics of the Code Phase Error for a Coherent DLL Tracking LTE Signals

In this section, the statistics of a coherent baseband discriminator output for LTE signals are derived through open-loop analysis. Subsequently, the statistics of the code phase error resulting from using a DLL with a coherent baseband discriminator are derived through closed-loop analysis.

ISBN 978-0-9928626-7-1 © EURASIP 2017

A. Open-Loop Analysis

The coherent baseband discriminator function is defined as

$$D_k \triangleq Z_{E_k} - Z_{L_k} = (S_{E_k} - S_{L_k}) + (N_{E_k} - N_{L_k}).$$

The signal component of the discriminator function $S_{E_k} - S_{L_k}$ is shown in Fig. 2 for $t_{eml} = \{0.25, 0.5, 1, 1.5, 2\}$.

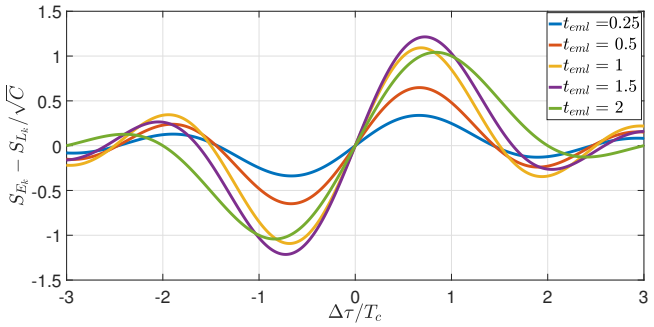

Fig. 2. Output of the coherent baseband discriminator function for the SSS with different correlator spacing.

It can be seen from Fig. 2 that the discriminator function can be approximated by a linear function for small values of $\Delta\tau_k$, as given by

$$D_k = k_{SSS}\Delta\tau_k + N_{E_k} - N_{L_k}, \tag{1}$$

where k_{SSS} is the slope of the discriminator function at $\Delta\tau_k = 0$, which is obtained by

$$k_{SSS} = \left.\frac{\partial D_k}{\partial \Delta\tau_k}\right|_{\Delta\tau_k=0} = 4\sqrt{C}W_{SSS}\left(2\frac{\sin(\pi t_{eml}/2)}{\pi t_{eml}^2} - \frac{\cos(\pi t_{eml}/2)}{t_{eml}}\right).$$

The mean and variance of D_k can be obtained from (1) as

$$\mathbb{E}\{D_k\} = k_{SSS}\Delta\tau_k, \tag{2}$$

$$\mathrm{var}\{D_k\} = \frac{N_0}{T_{sub}}\left[1 - R(t_{eml}T_c)\right]. \tag{3}$$

B. Closed-Loop Analysis

In a rate-aided DLL, the pseudorange rate estimated by the FLL-assisted PLL is added to the output of the DLL discriminator. In general, it is enough to use a first-order loop for the DLL loop filter since the FLL-assisted PLL's pseudrange rate estimate is accurate. The closed-loop error time-update for a first-order loop is shown to be [19]

$$\Delta\tau_{k+1} = (1 - 4B_L T_{sub})\Delta\tau_k + K_L D_k,$$

where B_L is the loop noise-equivalent bandwidth and K_L is the loop gain. To achieve the desired loop noise-equivalent bandwidth, K_L must be normalized according to

$$K_L = \left.\frac{4B_L T_{sub}\Delta\tau_k}{\mathbb{E}\{D_k\}}\right|_{\Delta\tau_k=0}.$$

Using (2), the loop noise gain for a coherent baseband discriminator becomes $K_L = \frac{4B_L T_{sub}}{k_{SSS}}$.

Assuming zero-mean tracking error, i.e., $\mathbb{E}\{\Delta\tau_k\} = 0$, the variance time-update is given by

$$\mathrm{var}\{\Delta\tau_{k+1}\} \triangleq (1 - 4B_L T_{sub})^2 \mathrm{var}\{\Delta\tau_k\} + K_L^2 \mathrm{var}\{D_k\}.$$

At steady state, $\mathrm{var}\{\Delta\tau\} = \mathrm{var}\{\Delta\tau_{k+1}\} = \mathrm{var}\{\Delta\tau_k\}$; hence,

$$\mathrm{var}\{\Delta\tau\} = \frac{B_L\, g(t_{eml})}{8(1 - 2B_L T_{sub})W_{SSS}^2 C/N_0}, \tag{4}$$

$$g(t_{eml}) \triangleq \frac{[1 - \mathrm{sinc}(t_{eml})]}{\left[2\frac{\sin(\pi t_{eml}/2)}{\pi t_{eml}^2} - \frac{\cos(\pi t_{eml}/2)}{t_{eml}}\right]^2}.$$

From (4), it can be seen that the standard deviation of the ranging error is related to the correlator spacing through $g(t_{eml})$. Fig. 3 shows $g(t_{eml})$ for $0 \le t_{eml} \le 2$. It can be seen that $g(t_{eml})$ is not a linear function, and it increases significantly faster when $t_{eml} > 1$. Therefore, to achieve a relatively high ranging precision, t_{eml} must be set to be less than 1. It is worth mentioning that for the GPS C/A code with an infinite bandwidth, $g(t_{eml}) = t_{eml}$.

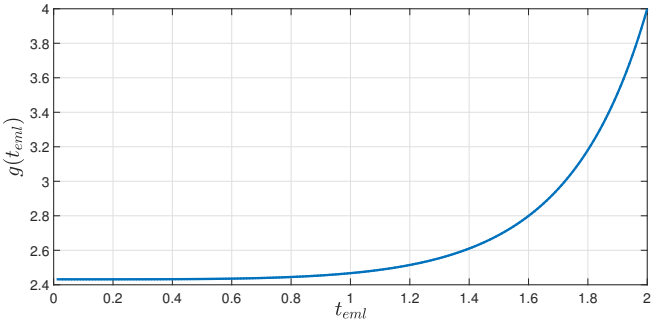

Fig. 3. The standard deviation of the ranging error $\Delta\tau$ is related to the correlator spacing through $g(t_{eml})$, which is shown as a function of t_{eml}.

Fig. 4 shows the pseudorange error of a coherent DLL as a function of the carrier-to-noise ratio (C/N_0), with $B_L = \{0.005, 0.05\}$ Hz and $t_{eml} = \{0.25, 0.5, 1, 1.5, 2\}$. It is worth mentioning that in Fig. 4, the bandwidth is chosen to be $B_L = \{0.005, 0.05\}$ Hz to enable the reader to compare the results with the standard GPS results provided in [22].

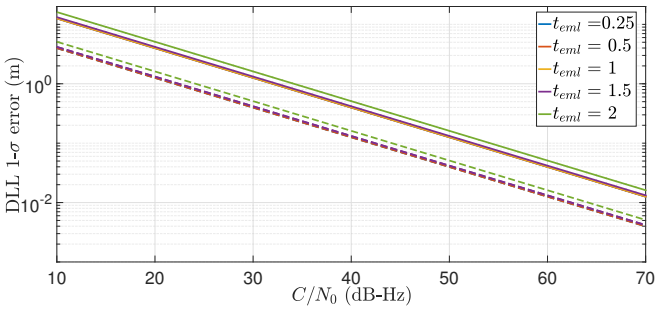

Fig. 4. Coherent baseband discriminator noise performance as a function of C/N_0, for different t_{eml} values. Solid and dashed lines represent the results for $B_L = 0.05$ Hz and $B_L = 0.005$ Hz, respectively.

While the ranging accuracy of a coherent baseband DLL was evaluated in the presence of white noise, other sources of

ISBN 978-0-9928626-7-1 © EURASIP 2017

errors may affect the ranging accuracy. The effect of multipath, which is another significant source of error is discussed next.

IV. Code Phase Error Analysis in Multipath Environments

In general, a multipath channel can be modeled as

$$h(s,t) = \sum_{l=0}^{L-1} \alpha_l(t)\delta(s - \tau_l(t)),$$

where $\alpha_l(t)$ and $\tau_l(t)$ are the path complex gain and delay of the l-th path at time t, respectively, δ is the Dirac delta function, and L is the total number of paths. Therefore, the received signal at the receiver can be expressed as

$$r(t) = \sum_{l=0}^{L-1} \alpha_l(t)y(t - \tau_l(t)) + n(t), \tag{5}$$

where $y(t)$ is the transmitted data. Subsequently, the signal components of the early and late correlations are given by

$$S_{E_k} = \sqrt{C}\sum_{l=0}^{L-1} \alpha_l(t)R\big[\Delta\tau_k - \frac{t_{eml}}{2}T_c - \tau_l(t)\big],$$

$$S_{L_k} = \sqrt{C}\sum_{l=0}^{L-1} \alpha_l(t)R\big[\Delta\tau_k + \frac{t_{eml}}{2}T_c - \tau_l(t)\big].$$

The discriminator function may be attenuated in a multipath channel, and the amount of attenuation depends on α_l and τ_l. In general, obtaining a closed-form expression for the pseudorange error from the DLL in a multipath environment is intractable. In this section, the performance of a DLL tracking the SSS code phase with a coherent discriminator is characterized numerically. The considered scenario assumes a channel with only one multipath component with $\alpha_0 = 1$ and $\alpha_1 = 0.2512e^{j\phi}$ (i.e., the multipath amplitude is 6 dB lower than the line-of-sight (LOS) amplitude). The effect of the delay of the reflected signal (τ_1) on the pseudorange estimation performance is evaluated for $\phi = \{0, \pi\}$, i.e., for constructive and destructive interference, respectively. Moreover, since the goal is to assess the ranging performance in a multipath environment, no noise was added to the simulated signals. The zero-crossing point of the discriminator function was calculated using Newton's iterative method. The resulting pseudorange error is shown in Fig. 5 as a function of the relative path delay (in meters) and for different t_{eml} values.

In what follows, some remarks outlining the major differences between a GPS and an LTE receiver employing a DLL with a coherent baseband discriminator are presented.

Remark 1. The autocorrelation function of the GPS C/A code with an infinite bandwidth has a triangular shape, which is zero-valued for time delays greater than T_c. Therefore, for $\tau_l > (1 + t_{eml}/2)T_c$, multipath does not introduce any errors in the pseudorange. However, the autocorrelation function of the SSS is a sinc function, which has non-zero values for time delays higher than $(1 + t_{eml}/2)T_c$. Consequently, there will always be multipath-induced pseudorange errors when tracking the SSS in multipath environments, even in the case of long-delay multipath (see Fig. 5).

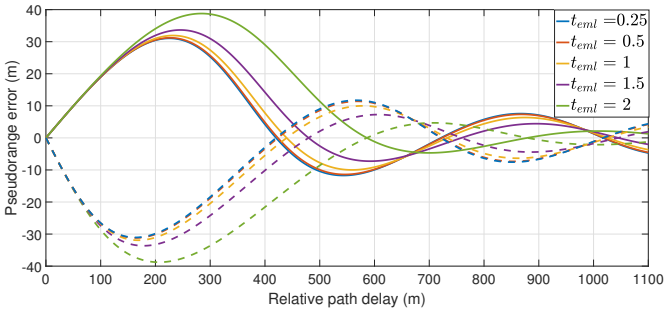

Fig. 5. Pseudorange error for a channel with one multipath component with an amplitude that is 6 dB lower than the amplitude of the LOS signal. The error is plotted as a function of the path delay (in meters) and for different t_{eml} values. The solid and dashed lines represent constructive and destructive interferences, respectively.

Remark 2. In a GPS receiver with an infinite bandwidth in a noise-free environment, decreasing the correlator spacing, t_{eml}, always reduces the pseudorange error. In practice, due to the band-limiting effect of the receiver, the correlator spacing should be greater than the reciprocal of the receiver bandwidth. In an LTE receiver, on the other hand, decreasing the correlator spacing may either (1) reduce the pseudorange error if the signal is subject to channel noise only or if it is in a short-delay multipath environment or (2) increase the pseudorange error if the receiver is in a long-delay multipath environment.

In summary, multipath causes pseudorange errors in an SSS-based LTE navigation receiver. It is worth noting that in LTE, the CRS may be used to improve the ranging accuracy in multipath environments. It is shown in [18] that the error due to multipath can be significantly decreased by detecting the first peak of the estimated channel impulse response.

V. Experimental Results

To demonstrate the analytical expression of the SSS ranging precision obtained in Section III-B versus experimental values, a field test was conducted with real LTE signals for a steady-state receiver. For this purpose an unmanned aerial vehicle (UAV) was equipped with an Ettus E312 universal software radio peripheral (USRP), a consumer-grade tri-band omnidirectional antenna, and a consumer-grade GPS antenna to acquire and track LTE signals at a sampling frequency of 3 MHz. The LTE SDR proposed in [18] was used to acquire and track the recorded LTE signals. The correlator spacing and the DLL loop filter bandwidth were set to be $t_{eml} = 1$ and $B_L = \{0.005, 0.05\}$ Hz, respectively. The PLL and FLL bandwidths were set to be 8 and 0.01 Hz, respectively. The test was performed over 60 seconds, collecting 6000 samples after steady-state. Fig. 6 shows the experimental setup.

The analytical value of the standard deviation of the ranging error was calculated according to (4), in which it is assumed that the receiver is stationary. Therefore, the UAV was set to hover in a clear LOS, while varying its distance to the eNodeB in order to vary the $C/N0$. The experimental results are shown in Fig. 7.

ISBN 978-0-9928626-7-1 © EURASIP 2017

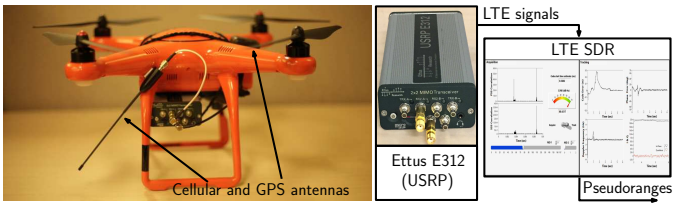

Fig. 6. Experimental setup.

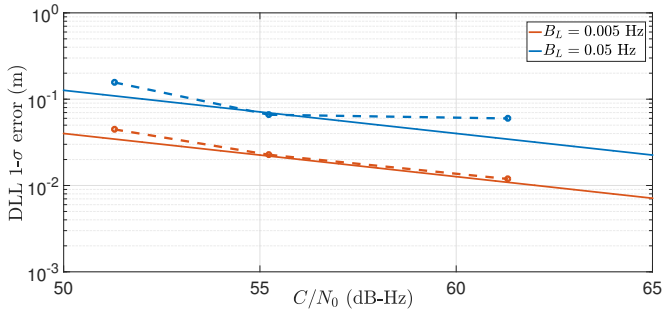

Fig. 7. Standard deviation of ranging with LTE SSS signal comparing the analytical and experimental results. Solid and dashed lines represent the analytical and experimental results, respectively.

It can be seen from Fig. 7 that the experimental ranging error standard deviation follows very closely the analytical expression derived in (4). The small discrepancies between the experimental and analytical values are attributed to several factors including: (1) the residual carrier phase and Doppler frequency being not completely negligible and (2) at a very long distance between the UAV and the eNodeB, corresponding to low C/N_0, the measured ranging error standard deviation will be higher than the theoretical value due to interference, quantization, and unmodeled effects, which are not captured by the derived analytical expression.

VI. Conclusion

The SSS ranging error in the presence of additive white noise and multipath was analyzed for LTE systems. A closed-form expression for the ranging error standard deviation was derived for a DLL with a coherent baseband discriminator. Moreover, the effect of multipath on the ranging error was studied numerically, and it was concluded that, in contrast to GPS, a larger correlator spacing reduces the pseudorange error in the presence of long-delay multipath. Experimental results closely matching the analytical expression of the standard deviation of pseudorange error were presented. Remarks outlining the major differences between a GPS and LTE receiver were also presented.

Acknowledgment

This work was supported in part by the Office of Naval Research (ONR) under Grant N00014-16-1-2305.

References

[1] K. Pesyna, Z. Kassas, J. Bhatti, and T. Humphreys, "Tightly-coupled opportunistic navigation for deep urban and indoor positioning," in *Proceedings of ION GNSS Conference*, September 2011, pp. 3605–3617.

[2] C. Yang, T. Nguyen, and E. Blasch, "Mobile positioning via fusion of mixed signals of opportunity," *IEEE Aerospace and Electronic Systems Magazine*, vol. 29, no. 4, pp. 34–46, April 2014.

[3] J. Khalife, K. Shamaei, and Z. Kassas, "A software-defined receiver architecture for cellular CDMA-based navigation," in *Proceedings of IEEE/ION Position, Location, and Navigation Symposium*, April 2016, pp. 816–826.

[4] J. Morales, P. Roysdon, and Z. Kassas, "Signals of opportunity aided inertial navigation," in *Proceedings of ION GNSS Conference*, September 2016, pp. 1492–1501.

[5] J. Morales, J. Khalife, and Z. Kassas, "Collaborative autonomous vehicles with signals of opportunity aided inertial navigation systems," in *Proceedings of ION International Technical Meeting Conference*, January 2017, 805–818.

[6] ——, "GNSS vertical dilution of precision reduction using terrestrial signals of opportunity," in *Proceedings of ION International Technical Meeting Conference*, January 2016, pp. 664–669.

[7] ——, "Opportunity for accuracy," *GPS World Magazine*, vol. 27, no. 3, pp. 22–29, March 2016.

[8] J. del Peral-Rosado, J. Lopez-Salcedo, G. Seco-Granados, F. Zanier, and M. Crisci, "Preliminary analysis of the positioning capabilities of the positioning reference signals of 3GPP LTE," in *Proceedings of European Workshop on GNSS signals and Signal Processing*, December 2011.

[9] ——, "Achievable localization accuracy of the positioning reference signal of 3GPP LTE," in *Proceedings of International Conference on Localization and GNSS*, June 2012, pp. 1–6.

[10] ——, "Evaluation of the LTE positioning capabilities under typical multipath channels," in *Proceedings of Advanced Satellite Multimedia Systems Conference and Signal Processing for Space Communications Workshop*, September 2012, pp. 139–146.

[11] F. Knutti, M. Sabathy, M. Driusso, H. Mathis, and C. Marshall, "Positioning using LTE signals," in *Proceedings of Navigation Conference in Europe*, April 2015, pp. 1–8.

[12] M. Driusso, F. Babich, F. Knutti, M. Sabathy, and C. Marshall, "Estimation and tracking of LTE signals time of arrival in a mobile multipath environment," in *Proceedings of International Symposium on Image and Signal Processing and Analysis*, September 2015, pp. 276–281.

[13] M. Ulmschneider and C. Gentner, "Multipath assisted positioning for pedestrians using LTE signals," in *Proceedings of IEEE/ION Position, Location, and Navigation Symposium*, April 2016, pp. 386–392.

[14] M. Driusso, C. Marshall, M. Sabathy, F. Knutti, H. Mathis, and F. Babich, "Vehicular position tracking using LTE signals," *IEEE Transactions on Vehicular Technology*, vol. 66, no. 4, pp. 3376–3391, April 2017.

[15] J. del Peral-Rosado, J. Lopez-Salcedo, G. Seco-Granados, F. Zanier, P. Crosta, R. Ioannides, and M. Crisci, "Software-defined radio LTE positioning receiver towards future hybrid localization systems," in *Proceedings of International Communication Satellite Systems Conference*, October 2013, pp. 14–17.

[16] J. del Peral-Rosado, J. Parro-Jimenez, J. Lopez-Salcedo, G. Seco-Granados, P. Crosta, F. Zanier, and M. Crisci, "Comparative results analysis on positioning with real LTE signals and low-cost hardware platforms," in *Proceedings of Satellite Navigation Technologies and European Workshop on GNSS Signals and Signal Processing*, December 2014, pp. 1–8.

[17] K. Shamaei, J. Khalife, and Z. Kassas, "Performance characterization of positioning in LTE systems," in *Proceedings of ION GNSS Conference*, September 2016, pp. 2262–2270.

[18] ——, "Comparative results for positioning with secondary synchronization signal versus cell specific reference signal in LTE systems," in *Proceedings of ION International Technical Meeting Conference*, January 2017, 1256–1268.

[19] A. van Dierendonck, P. Fenton, and T. Ford, "Theory and performance of narrow correlator spacing in a GPS receiver," *Journal of the Institute of Navigation*, vol. 39, no. 3, pp. 265–283, September 1992.

[20] 3GPP, "Evolved universal terrestrial radio access (E-UTRA); physical channels and modulation," 3rd Generation Partnership Project (3GPP), TS 36.211, January 2011. [Online]. Available: http://www.3gpp.org/ftp/Specs/html-info/36211.htm

[21] M. Braasch and A. van Dierendonck, "GPS receiver architectures and measurements," in *Proceedings of the IEEE*, vol. 87, no. 1, January 1999, pp. 48–64.

[22] P. Misra and P. Enge, *Global Positioning System: Signals, Measurements, and Performance*, 2nd ed. Ganga-Jamuna Press, 2010.